Journal of Membrane Science 427 (2013) 336–344

Contents lists available at SciVerse ScienceDirect

Journal of Membrane Science

journal homepage: www.elsevier.com/locate/memsci

Fabrication of nanofiber meltblown membranes and their filtration properties

Mohammad Abouelreesh Hassan [a], Bong Yeol Yeom [b], Arnold Wilkie [c], Behnam Pourdeyhimi [b,*], Saad A. Khan [a,**]

[a] Department of Chemical and Biomolecular Engineering, North Carolina State University, Raleigh, NC 27695-7905, USA
[b] The Nonwovens Institute, North Carolina State University, Raleigh, NC 27695-8301, USA
[c] Hills Inc., West Melbourne, FL 32904-1195, USA

ARTICLE INFO

Article history:
Received 19 May 2012
Received in revised form
7 September 2012
Accepted 15 September 2012
Available online 7 October 2012

Keywords:
Nanofibers
Meltbowing
Filtration
Nonwoven membranes
HEPA filters

ABSTRACT

Meltblowing is a unique one-step process for producing self-bonded fibrous nonwoven membranes directly from polymer resins, with average fiber diameter ranging between 1 and 2 μm. Determining routes for making nano- or submicron-fibers using this process are desirable since there are many manufacturing assets that are already in place. It is envisaged that these nonwoven membranes will find applications in critical areas such as medical, hygiene, filtration, bioseparation, and others. In this study, we investigate the influence of different die configurations and operating conditions on fiber and web characteristics. We also report on strategies for reducing the fiber size below one micron to achieve higher filtration quality at lower basis weight relative to the conventional meltblown webs. Their performance is compared to a control meltblown sample produced by using a typical die design. We find that production of nano-meltblown membranes with an average fiber size in the range of 300–500 nm using this new die design is possible and report on process operating conditions that result in such structures. These samples achieve equal filtration efficiencies to that of our control sample at 88% reduced basis weight but at a lower polymer throughput. The lower basis weight also resulted in a lower pressure drop and overall, the new samples exhibited a higher quality factor, twice that of the control. These results show significant promise for the use of nano-meltblown fibers in filtration applications.

1. Introduction

Nanofibers membranes are an exciting class of materials that exhibit many desirable attributes primarily due to their extremely high surface to weight ratio, interconnected pore structure and high permeability for gases [1]. In particular, low density, large surface area to mass, high pore volume, and tight pore size qualify nanofibrous membranes to be useful for many filtration applications such as filtering submicron particles from air or water [1–3]. Nanofibers can also be utilized for applications in the aerospace industry and information technology, and in capacitors, transistors, drug delivery systems, battery separators, and energy storage devices and fuel cells [4].

Typically, nanofibers are produced using electrospinning, a process in which a charged fluid jet from a polymer solution or melt undergoes stretching and whipping in the presence of an applied electric field resulting in continuous ultrathin randomly oriented fibers in the form of a non-woven mat deposited on a collector [5–7]. These fibers have diameters in the range of 100–500 nm. Despite its simplicity and ability to produce functional nanofibers [7–10], the electrospinning process is inherently slow and solvent intensive, and the choice of polymers used is limited. Melt-electrospinning has been an area of interest but no real success has been documented yet. Some published results indicate also that the average fiber diameters are quite large (35 ± 8 μm) and requires viscosity-reducing additive to lower the range to a more acceptable range of 840 ± 190 nm [11]. There is also significant interest in capitalizing on existing high throughput fiber spinning methods to produce nanofibers; this would combine both desirable facets into one existing process.

Almost all fiber barrier membranes used in the nonwovens industry are based on meltblowing technology, a melt spinning processes used to produce microfibers by injecting molten polymer streams into high velocity gas/air jets that form a self-bonded web when collected on a moving surface. Fig. 1 shows a schematic illustration of the process in which high-velocity air jets impinge upon the polymer as it emerges from the spinneret. The drag force caused by the air attenuates the fiber rapidly, and reduces its diameter by as much as hundred times from that of the nozzle

* Corresponding author. Tel.: +1 919 515 6551.
** Corresponding author. Tel.: +1 919 515 4519.
E-mail addresses: bpourdey@ncsu.edu (B. Pourdeyhimi), khan@eos.ncsu.edu (S.A. Khan).

0376-7388/$ - see front matter © 2012 Elsevier B.V. All rights reserved.
http://dx.doi.org/10.1016/j.memsci.2012.09.050

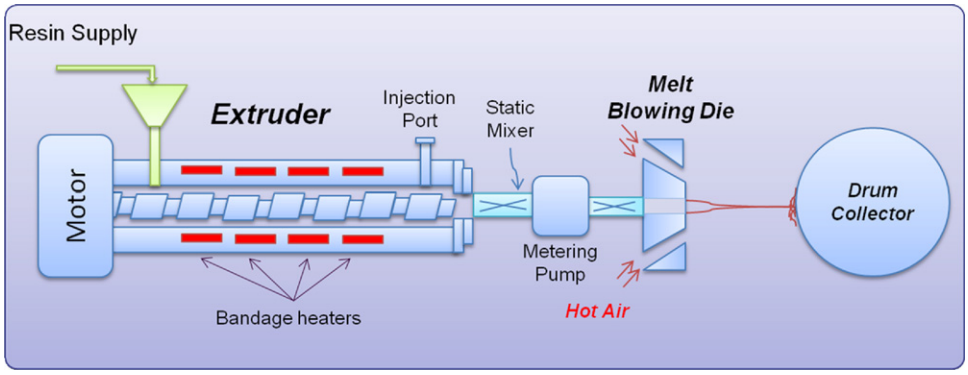

Fig. 1. Schematic drawing of the MB process.

diameter [12]. Typical meltblown membranes have fiber sizes ranging from 0.5 to 10 μm with an average fiber diameter of 1–2 μm. Meltblown webs are known for their high surface area per unit weight, high insulation value, and high barrier properties. These properties make them excellent candidates for making high quality filters, surgical drapes and gowns, diaper leg cuff, protective apparel where a barrier to fluids and breathability are essential features [13,14].

One critical area of application for meltblown webs is in the area of aerosol filtration. The advantages of small fibers for filtration are well documented [15]. Meltblowing has the potential to compete favorably with electrospinning if the meltblowing process could be used to produce materials in the nanofiber range; meltblowing would provide a much faster, easier, and less costly alternative to the electrospinning technique. It is not surprising that meltblowing has prompted a significant amount of activity in the literature. Investigators have studied the process from different perspectives. Several studies [16–26] have focused on characterizing the process–structure–property relationships by using techniques such as laser doppler velocimetry and high speed imaging and computational fluid dynamics. Shambaugh et al. [20–26] studied the effect of the slot die geometry on the air flow field below the MB die and its effect on the fiber size. The effect of the nose-piece shape on the flow field under the MB die was investigated experimentally by Tate and Shambaugh [21] and theoretically by using CFD simulations by Krutka and Shambaugh [24–26]. Tate et al. showed experimentally that using a blunt MB die produces a lower maximum centerline velocity and that the centerline velocity profile decays at a higher rate than that observed using a sharp MB die. Higher maximum centerline air velocity in the z-direction is favorable as it leads to an increased rate of fiber attenuation (i.e., finer fiber) for a given air flow rate. Milligan and Wadsworth [27] made use of a cross-flow to obtain finer fiber diameter and improve the uniformity of the produced fiber mats. Lee and Wadsworth [28] studied the effect of meltblowing process condition such as air temperature, die to collector distance, and air flow rate on filtration properties of meltblown polypropylene webs. They found that pore size and air permeability decreased with increasing processing temperature, increasing air flow rate at the die, or decreasing die-to-collector distance.

Some attempts have also been made to fabricate nano-meltblown fibers. Companies such as Arthur G. Russell designed laminated stainless steel dies to operate at high extrusion pressures ~1500 psi with 64 orifices/inch [29]. They showed the ability to produce fibers with an average diameter of 400 nm by using a 6 in. single raw die. However, they noted a lot of "fly" during the production. Fly refers to broken fiber debris that is air borne. Fly is mostly caused by very high air velocities that cause fiber breakage. Ward and Fabricante et al. [30,31] claimed to produce nanofibers with average size of 300 nm by using a new die design composed of stacked plates that form a row of orifices as small as 0.0125 mm in diameter but no data or SEM images for such fibers were provided. Ellison et al. [32] were able to produce some nanofibers with an average size of 500 nm by using a single hole die. This was achieved by lowering the throughput, increasing polymer temperature, and increasing the air flow rate (≈ 70 psi) while keeping the same spinneret diameter. Working at very high aspirator pressures may not be commercially acceptable because of defects such as rope formation and fly. Also, lowering the throughput significantly will result in large residence time in the extruder, creating the potential for polymer degradation.

The data and results in the literature seem to suggest that reduction in fiber size is possible, but no in-depth, or systematic study of fiber development, die configuration and concomitant effects on fiber size, web uniformity and filtration properties can be found. We report on strategies for forming nano-range meltblown fibers by using new die designs and by manipulating the processing parameters. The work was completed on a pilot scale meltblowing setup. Filtration properties, fiber and membrane characteristics of the resulting webs were examined and compared to a typical micro-range meltblown membrane produced using a typical MB die design.

2. Experimental

2.1. Pilot meltblowing unit

The webs were fabricated by using a pilot scale meltblowing set-up at Hills, Inc. Three 60 cm wide slot dies with different hole diameters and different inter-hole distances were used in this line. Since the 1960s, the slot die concept has been described in numerous patents [33–38]. Compressed air for blowing the molten polymer was routed first through an electric heater, and then fed by one hose on each side of the spin pack (i.e., one upstream and one downstream). Polymer pellets were melted and pressurized using a 1.9 cm extruder, mounted vertically with a special screw design for low viscosity polymers. The heating in the extruder involved four zone temperature controls; the first zone of the screw extruder was water-cooled, in order to minimize polymer degradation. The polymer used in the trials was a metallocene, isotactic polypropylene (Exxon, Achieve^{TM} 6936 G) with 1800 melt flow rate (MFR). The fibers were collected as a mat on a belt type collector (Albany International, 55 LD). Webs from the belt collector were collected onto rolls.

2.2. Die geometry

Three 60 cm wide stainless steel slot dies were used in the experimental study. A schematic illustration of the die is shown in Fig. 2 [38], and the design details are provided in Table 1.

The polymer orifices were spaced evenly across the central 50 cm. The control sample was produced using a regular meltblowing (MB) die (Die—Control) that has 681 holes with a hole density of 14 holes/cm. Die [A] has 1470 polymer capillaries with a hole density of 30 holes/cm, while die [B] has 1960 capillaries with hole density of 39 holes/cm. The die tip was sharp, i.e., mean radius was less than 0.127 mm. The angle between each of the air slots and the face of the die was 60°. The nosepiece was setback by 0.508 mm.

The new dies A and B have smaller diameters, and high L/D ratio that generate high pressure drop at low polymer throughput, and hence increase flow uniformity. In addition, the long holes contribute to the strength of the nozzle and therefore allow high operating pressures. Finally the smaller diameters allow increasing hole density to gain back some of the productivity that is lost because of working at low polymer throughput.

2.3. Operating conditions

The operating conditions were chosen to determine process windows that would produce sub-micron fibers that could potentially be used in manufacturing high quality membrane filters using the new die designs. The die temperature was set at 240 °C; air temperature was set at 280 °C. The die to collector distance (DCD) was set at 19 cm for Die [A] and 14 cm for Die [B]. The experimental conditions for the trials are shown in Tables 2 and 3. As shown in Table 2, the polymer throughput was varied between 0.214 and 0.0022 g/hole/min and the belt speed was kept constant at 14.85 m/min. One of the goals of conducting the trial of Group 1 was to produce nanofibers that can achieve similar filtration efficiency to a control microfiber sample at a lower basis weight. In Group 2, the web basis weight was varied at a relatively constant fiber diameter to examine the influence of basis weight on performance at constant fiber diameters.

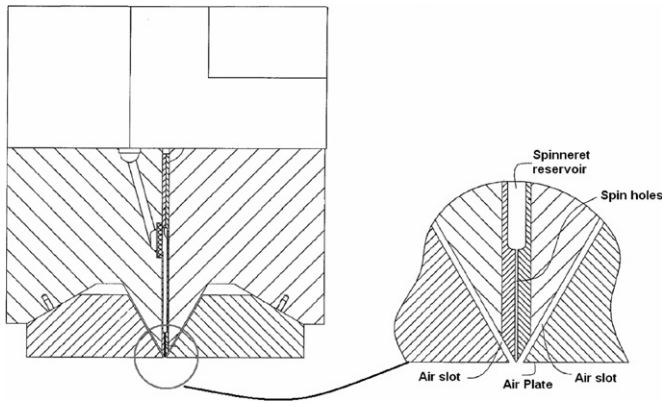

Fig. 2. Schematic illustration of the MB die, adapted from Ref. [38].

Table 1
Configuration of different dies.

Die type	L/D	Hole density (holes/cm)	Orifice diameter (mm)	Space between capillaries (mm)
Control	30	14	0.3048	0.3048
Die [A]	50	30	0.1778	0.1778
Die [B]	200	39	0.127	0.127

2.4. Fiber diameter measurements

To examine the fiber morphology, samples were sputter coated with a thin layer of gold and analyzed with a scanning electron microscope (SEM, FEI XL-30, FEI Co.). Images were taken at 10,000- × under 5 kV of an accelerating voltage for the electron beams. Fiber diameters were measured using Image *J* software. For each membrane, at least 100 individual fiber diameters were measured.

2.5. Air permeability measurements

The air permeability of a nonwoven membrane is the measured airflow through an area of filter media at a specified pressure drop. Using the Air Permeability Tester, Textest-FX3300 Labotester III, the air permeability was measured for the fiber mats under a drop pressure of 125 Pa. Some of the fabrics were layered in order to have a similar basis weight to allow easy comparison between samples. For each sample, 10 measurements were taken and averaged.

2.6. Filtration efficiency measurements

The filtration efficiency of the nonwoven membranes was examined by using the Automated Filter Tester, TSI 3160, that measures particle penetration versus particle size at a certain aerosol flow rate or face velocity. TSI 3160 generates two kinds of aerosol particles in the range of 10–800 nm, polydisperse dioctylphtalate (DOP), or NaCl, using an atomizer. TSI 3160 is capable of measuring efficiencies up to 99.999999% [39,40]. The filtration efficiency was measured by using dioctylphtalate (DOP) aerosol at a face velocity of 5.33 cm/s. Some samples were tested under three conditions: as-received, discharged, and charged. Samples were discharged by using isopropanol according to European standard EN-779. To charge our samples, we used a

Table 2
Group 1 processing conditions.

Sample	C	A1	A2	A3	A4	B1	B2
Polymer throughput (g/hole/min)	0.214	0.1	0.05	0.025	0.0125	0.0055	0.0022
Basis weight (g/m^2)	20	20	10	5	2.5	1.5	0.5
Belt speed (m/min)	15.6	14.85	14.85	14.85	15.5	14.5	14.5

Table 3
Group 2 processing conditions.

Sample	C	B1	B2	B3	B4
Polymer throughput (g/hole/min)	0.214	0.0055	0.002	0.002	0.002
Basis weight (g/m^2)	20	1.5	0.5	0.33	0.22
Belt speed (m/min)	15.6	14.5	14.5	22	33

Corona discharging technique and exposed the specimen for 10 min below the Corona discharging setup at 5 cm at 65% relative humidity and 20 °C. Full filtration curves for the samples were generated for particle sizes ranging from 0.02 to 0.4 μm.

2.7. Capillary flow porometry

A capillary flow porometer from Porous Materials Inc. (PMI, Ithaca NY) was used to analyze the pore structure of the nonwovens membranes. PMI porometry is based on the displacement of a wetting liquid from a pore by a gas [41] with the work done by the gas assumed to equal the interfacial increase in the free energy. The samples were tested with a Salwick wetting liquid that had a surface tension of 20.1 dynes/cm. It was assumed that Salwick completely wetted out the samples tested, and hence a contact angle of 0° was assumed for calculating pore diameter by using the Young–Laplace equation [42]: $D = \left(4\gamma_{L/G}\cos\theta\right)/p$

Here p is the extrusion pressure in MPa, D is the pore diameter in μm, $\gamma_{L/G}$ is the surface tension of Salwick in N/m and θ is the contact angle of Salwick with the sample, in degrees. This technique is capable of providing us with the pore diameter at the most constricted part of the pore, the bubble point diameter, as well as the pore diameter distribution.

3. Results & discussions

3.1. Fiber diameter

Fig. 3 shows the effect of polymer throughput on fiber diameter of meltblown membranes produced with different die designs. The average diameter varied from 0.3 μm to 1.5 μm. In general, we observe that as polymer throughput decreases, fiber diameter decreases. We also notice that Die [A] produced samples with fiber size similar to what could be produced by Die [B] (Fig. 3-Group 1) but at a higher polymer throughput which yields a higher production rate. The main reason behind this result is that the drag force is much higher in case of Die [A] because we are using higher aspirator pressures. Low aspirator pressure is used in the case of Die [B] to avoid fiber fly. Lowering polymer mass flow rate decreases fiber diameter because the same drag force from the air jet is acting on a smaller polymer mass.

Fig. 4 shows representative SEM images of the membranes and their fiber diameter distributions for Group 1 samples. In all cases, we find the fibers to be essentially shot-free. "Shot" refers to large particles of (molten) polymer (often several tens of microns in size) in the membrane that have ill-defined shapes [12]. From the histograms, we notice that the distribution of meltblown fiber is log-normal—this is common for meltblown structures. Fig. 5 shows another statistical representation of the fiber diameter distribution which is the box and whisker plots for the fabricated nonwoven membranes in Groups 1 and 2. The bottom and top of the box are the 25th and 75th percentile (the lower and upper quartiles, respectively), the solid band near the middle of the box is the 50th percentile (the median), while the dashed band represents the mean fiber diameter. Whiskers (error bars) above and below the box indicate the 90th and 10th percentiles. It is evident from Fig. 5 that for Group 2, the average fiber diameter of the samples is relatively constant at 0.45 ± 0.05 μm. In general, the resultant fiber diameters are consistent with the expectation of commercial webs (1–2 μm) or substantially smaller (0.3–1 μm) depending on the used die and processing conditions. These data show that it is feasible to significantly decrease the average fiber diameter below 1 μm by modulating processing parameters. The important findings that we need to emphasis here is that under some operating conditions, we are able to produce nonwovens membranes with an average fiber size $\approx$ 330 nm with a production rate of 2.23 kg/h/m of die width, which puts the meltblowing process with these new die designs as a viable technique to produce nanofibers with relatively high productivity compared to electrospinning. The production rate of the commercial electrospinning is around 650 kg/year in the case of Nylon 6 nanofibers at an average fiber diameter of 200 nm when producing webs in the range of 5 g/m^2 [43]. The production rate of a nano-meltblowing line of the same width (1.6 m) would be 26,750 kg/year (based on 8000 h/year) of polypropylene fabric produced at 2.5 g/m^2 with 330 nm as fiber diameter, a 40-fold increase in throughput from electrospinning.

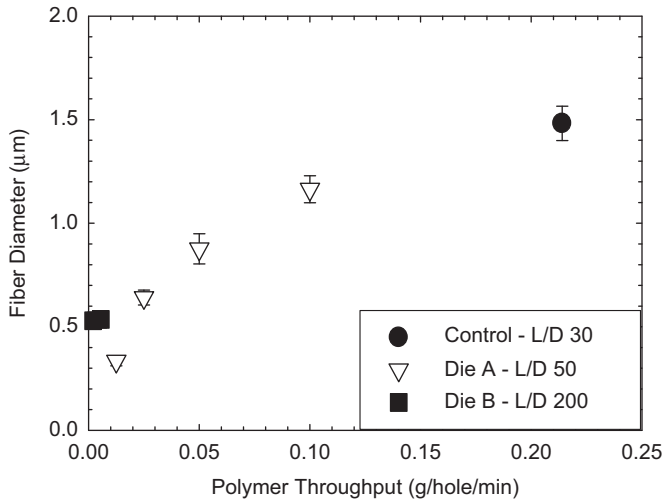

Fig. 3. Fiber diameter of meltblown membranes as a function of polymer throughput for different die designs. Results are shown for Group 1 samples.

3.2. Air permeability

Airflow through nonwovens membranes can be described with the channel theory that assumes that porous media is a bundle of cylindrical tubes passing from one surface of the media to the other surface, and not necessarily perpendicular to the surfaces [43]. Air permeability is inversely proportional to membrane thickness that is a function of web basis weight, as seen in Group 2 of Fig. 6. Air permeability can also be decreased by decreasing membrane pore size by decreasing the fiber diameter. The effect of basis weight and fiber diameter on air permeability can be seen as a competition where the more dominant component will dictate the overall trend. This correlation can be seen in Group 1 of Fig. 6 where the air permeability of the nonwovens membranes of die [A] samples are slightly increasing due to the competing effect of these two parameters, but the membranes that are produced by die [B] have relatively much higher air permeability due to the extremely lower basis weight compared to other membranes of Die [A] beside their comparable fiber diameters to that of samples A3 and A4. Thus the air permeability increase due to their lower basis weight is more dominant than the decrease that is due to the fiber diameter reduction.

The general conclusion that can be extracted here is that air permeability of fabrics could be tailored according to the web basis weight and the fiber size. As fiber size decreases, the pore size decreases and hence air permeability decreases if we have the same basis weights. Higher air permeability is desirable in filtration as it is inversely proportional to pressure drop.

3.3. Filtration efficiency

Our initial effort focused on the filtration efficiency of the as-received samples, in particularly determining whether we

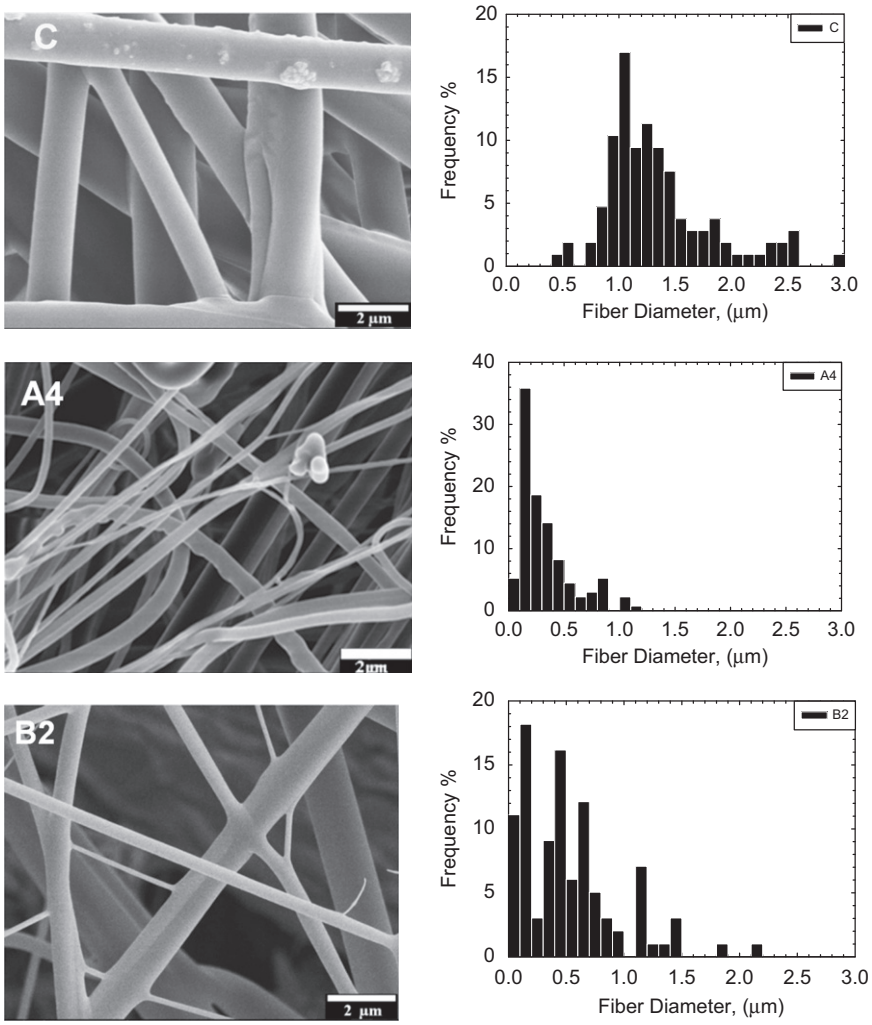

Fig. 4. SEM images of C, A4, and B2 samples (see Table 2 for details) and their fiber diameter distribution.

were dealing with mechanical efficiency only or a combination of mechanical and electrostatic efficiencies. To this end, the penetration % of three samples at two different conditions, as-received and discharged were measured. It is worth noting that some processes create charge in the samples due to mostly frictional effects. Discharging was done to ensure that the webs did not have any charge and that the filtration efficiency was only mechanical.

Fig. 7 shows differences between the penetration % for the as-received samples and the discharged samples. We observe the difference to be sufficiently small to be neglected, so that we can treat the as-received samples as if they are discharged samples due to the low electrostatic charges that they have. In other words, the reported filtration efficiency of the as-received samples can be considered as the mechanical efficiency only, because the filtration efficiency due to electrostatic charges in the as-received samples are negligible. This also means that our process did not induce any electrostatic charge.

Fig. 8a shows the filtration efficiency of Group 1 samples. Nonwoven membranes were challenged with 0.3 μm DOP aerosol at a face velocity of 5.3 cm/s. We find that samples produced by using Die [A] have relatively similar filtration efficiencies to that of the control sample although they were produced at a lower basis weight. The two samples that were produced by Die [B] have lower filtration efficiency relative to the control sample as they were produced at a much lower basis weight. The samples were therefore, expected to have very different pressure drops. In order to compare samples that differ in basis weights, pressure drop, and efficiency, the filtration quality factor (Q_f), sometimes called the figure of merit, has been calculated, and is shown in Fig. 8b. The filtration quality factor is defined as [44,45]

$$Q_f = \frac{fractional\ capture\ per\ unit\ thickness}{pressure\ drop\ per\ unit\ thickness} = \frac{\gamma}{\Delta p/h} = \frac{-ln\mathrm{P}}{\Delta p}$$

where $\gamma = E_\Sigma d_f L$, P is the penetration fraction, Δp is the pressure drop across the medium, E_Σ is the summation of different single-fiber efficiency mechanism, L is the filter thickness and d_f is the fiber diameter.

The filtration quality factor of web A4 is twice the Q_f of the control meltblown web. Even membranes B1 and B2 that exhibited lower filtration efficiencies relative to that of the control have much higher filtration quality factors.

Fig. 9 shows the filtration performance of Group 2 webs. Group 2 webs were produced at a relatively constant fiber diameter using Die [B] at different basis weights. The membranes show high filtration quality factor relative to the control sample although their filtration efficiency is much lower relative to the control sample. The higher quality factor is mainly due to the lower basis weight and pressure drop.

Fig. 10 shows the particle penetration fraction of layered samples of Group 1 versus the pressure drop across the filter media in a log–log plot. We find that the A4 sample reaches

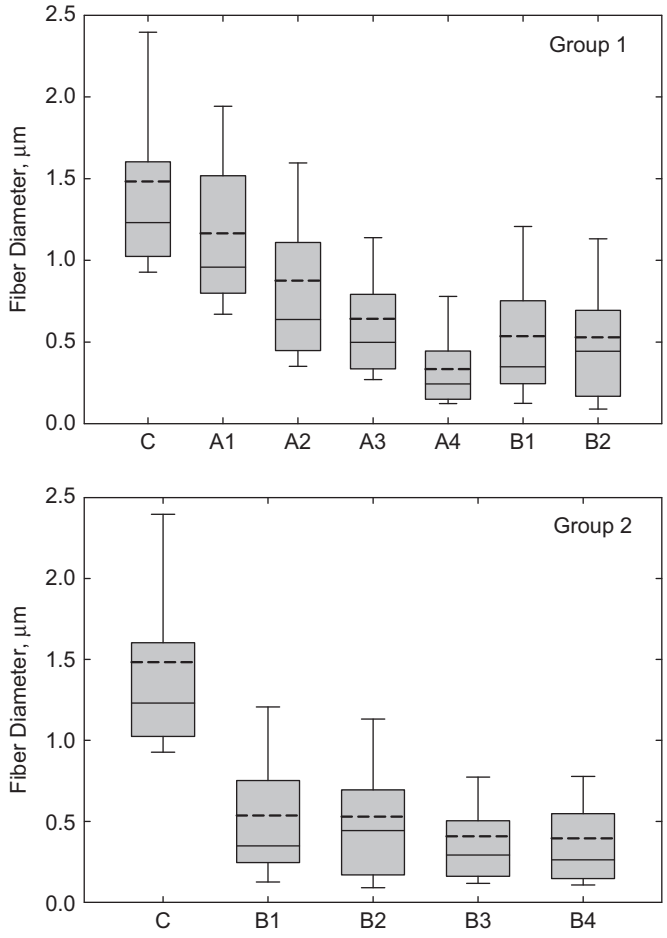

Fig. 5. Fiber diameter of nanoMB webs in Groups 1 and 2. The boundaries of the boxes indicate the 25th and the 75th percentiles and a straight and a dashed lines mark the median and the average fiber diameters. The error bars on the bottom and the top of the box indicate 10th and 90th percentiles.

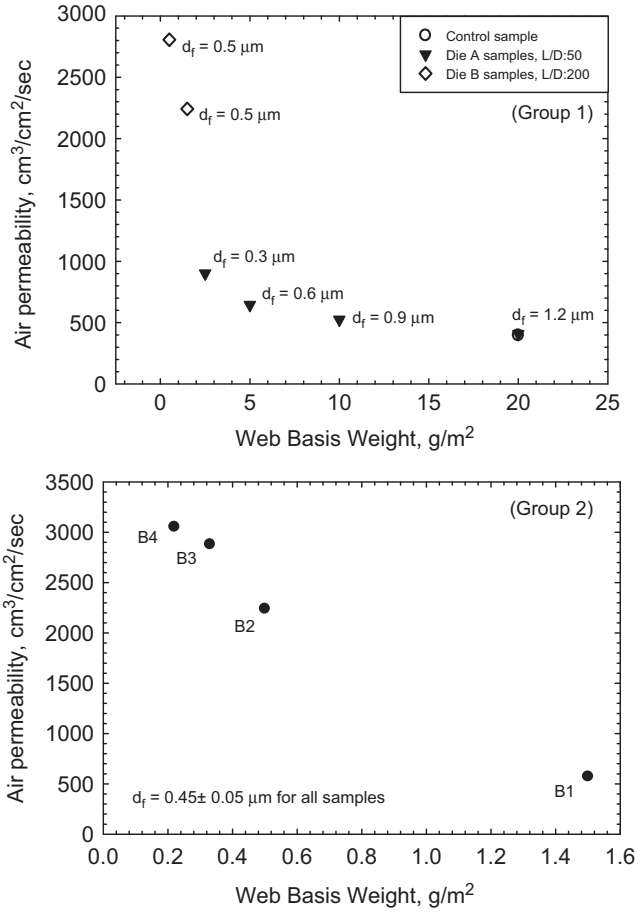

Fig. 6. Air permeability vs. basis weight for Groups 1 and 2.

HEPA-H14 filtration performance (99.978% mechanical efficiency at 280 Pa pressure drop) at 40 g/m^2. The fiber glass HEPA-H14 filter media provide the same filtration efficiency at similar pressure drop but at a higher basis weight.

The slope of the linear regression lines of each sample in Fig. 10 can be correlated to the filtration quality factor (Q_f) to give an average factor. For example sample A1 has a $(Q_f)_{avg}$ of 13.6, whereas sample A4 has a $(Q_f)_{avg}$ of 26. As shown, the smaller fiber diameter membranes (e.g., A4 samples) have higher slopes that result in a higher figure of merit. The superior properties of sample A4 to other samples goes back to the fact that it has sub-micron fibers.

Fig. 11 depicts the full filtration curves of discharged samples of Group 1. The aim of this test was to determine the most penetrating particle size (MPPS). Weight per unit area of all samples was kept constant at 20 g/m^2, and all membranes were challenged with DOP aerosols in size range of 0.02–0.40 μm at 5.3 cm/s face velocity. As seen from Fig. 11a, sample A4 provides the lowest MPPS values that are smaller than the control sample by more than one decade. This can again be attributed primarily to the size of the fibers. Fig. 11b shows the MPPS for the nonwoven membrane samples. We find the MPPS of the control sample to be the highest, whereas that of sample A4 to be the lowest, suggesting that the filtration efficiency at the MPPS of the control sample has been increased and shifted to a lower value. The reason behind this is the fiber size and the resultant smaller pore structure. The resultant MPPS values are consistent with

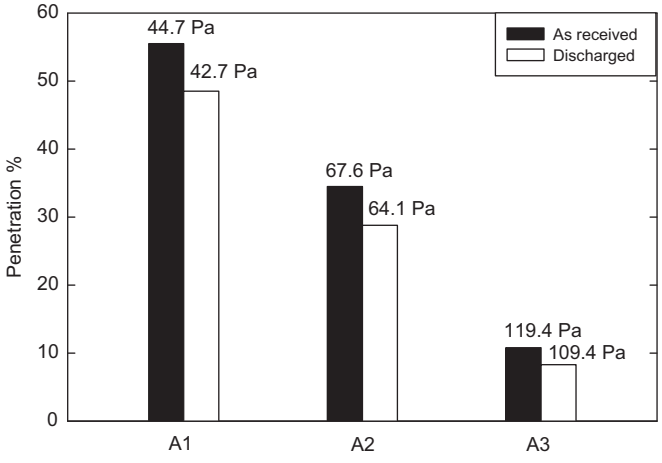

Fig. 7. Discharged vs. as-received penetration and pressure drop data for three samples.

what could be found in the literature which varies between 0.1 and 0.3 μm according to the membrane average fiber size [46].

3.4. Pore diameter analysis

Fig. 12 shows the average pore size and the bubble point diameter versus membrane basis weight for samples produced with Die [A]. We find that the samples exhibit a similar average pore diameter of ~7.5 μm although the fiber diameter is

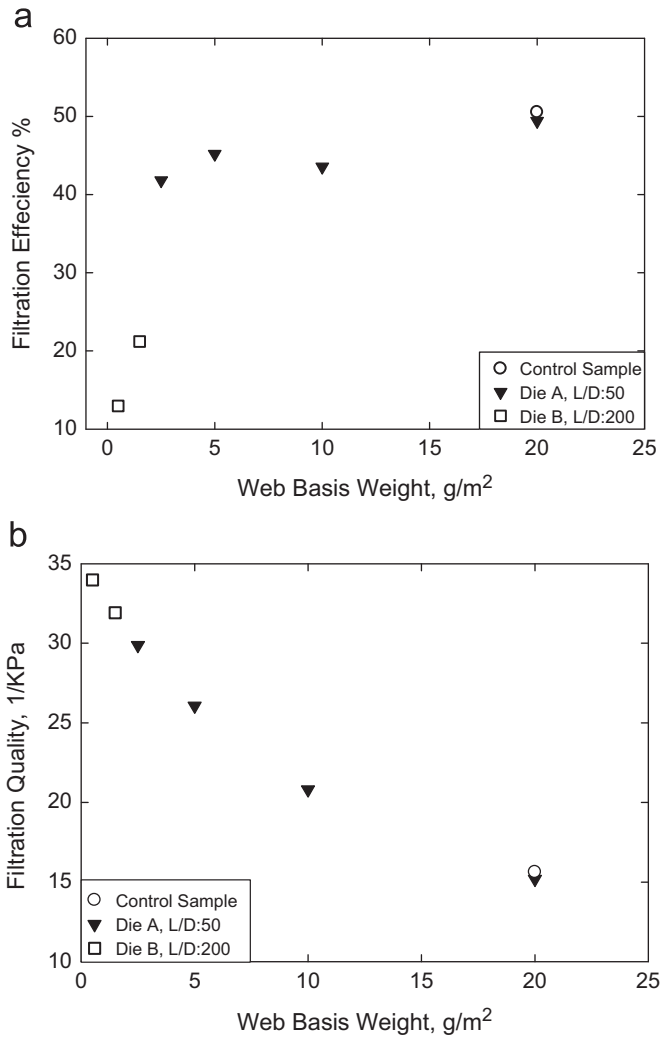

Fig. 8. Filtration efficiency (a) and filtration quality factor of Group 1 samples (b) vs. basis weight.

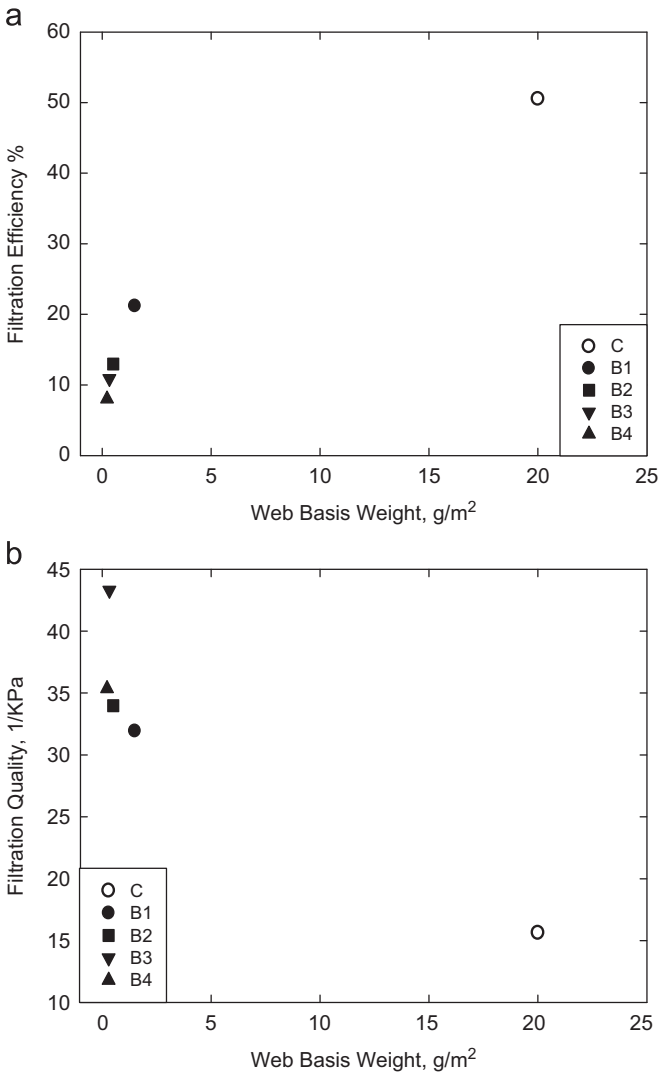

Fig. 9. Filtration efficiency (a) and filtration quality factor (2) vs. basis weight for Group 2 samples.

decreasing from sample A1 to A4. This is interesting as we would have anticipated a smaller pore size with decreasing fiber diameter [47]. The main reason behind this unusual trend is potentially that our membranes have different basis weights, therefore, the effect of fiber diameter on pore size is negated by the lower basis weight of the membranes. The similarity in pore size perhaps explains why we also achieved similar filtration efficiencies for our nanofibrous membranes compared with the control sample—the control had larger fibers and was heavier.

The results for the bubble point diameter which represents the largest pore diameter show a similar trend (Fig. 12), with a bubble point diameter for the samples of ~17.3 μm. However, the throat diameter which represents the smallest pore diameter is increasing with decreasing basis weight and this explains why we have lower filtration resistance or pressure drop for such nanofibrous membranes that has lower basis weight and smaller fiber diameters (see Supplementary Fig. 1).

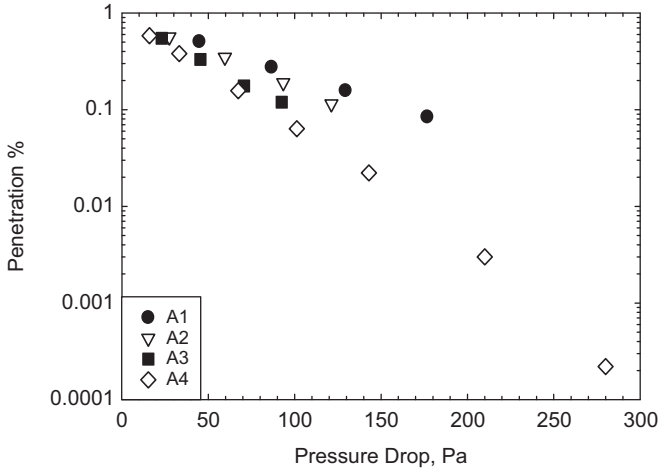

Fig. 10. Filtration performance of layered nano-meltblown webs (up to four layers for A1–A3, and up to six layers for A4) against 0.30 μm of DOP aerosol at 5.3 cm/s of face velocity.

4. Conclusions

We investigated the characteristics of nano-meltblown fibrous membranes produced by using three different die designs and different process conditions. We showed the possibility of producing nanofibers by using the meltblowing process at high production rate relative to the other techniques that produces nanofibers. We found that some of the nano-meltblown membranes that are produced using the new dies provide similar

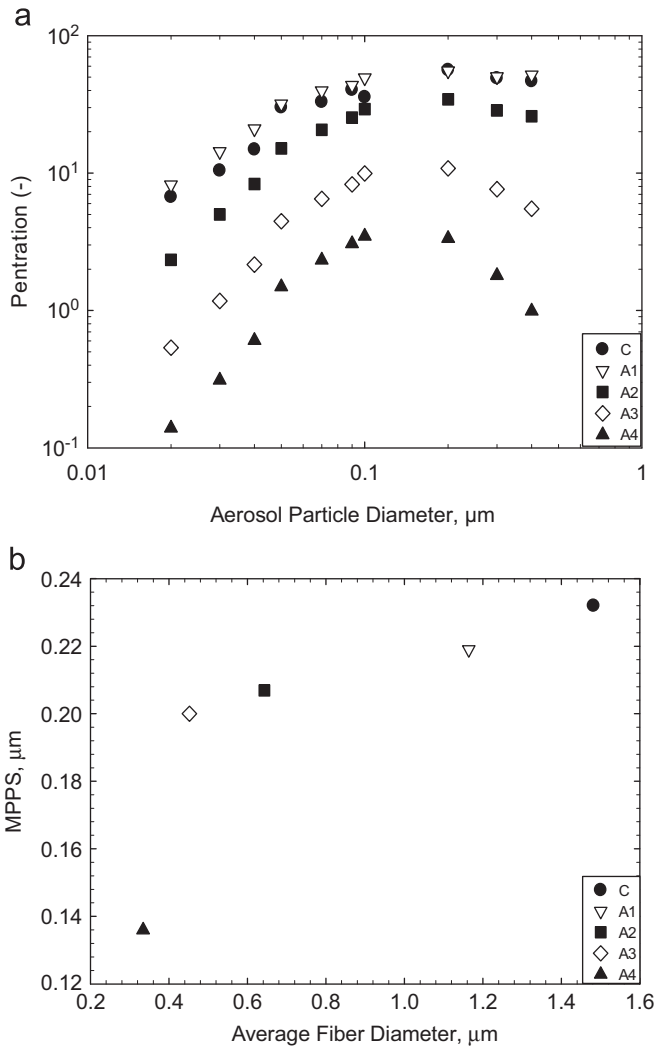

Fig. 11. Fractional penetration curve of nanoMB webs as-received (a) and corona charged (b) against DOP aerosols in size range of 0.02–0.40 μm at 5.3 cm/s of face velocity. Basis weight of all samples was 20 g/m^2.

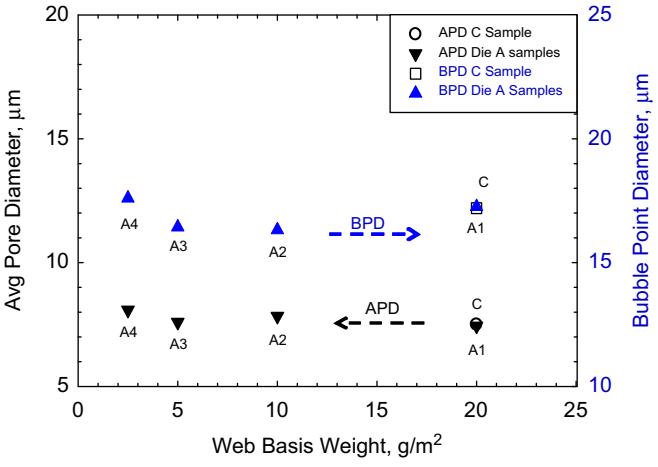

Fig. 12. Average pore diameter (APD), and Bubble point diameter (BPD) as a function of basis weight for Die A nonwovens membranes and the control sample.

filtration efficiencies at much lower basis relative to a control sample, and its filtration quality factor can be enhanced by more than 100% in some cases without affecting the yardage production. We also demonstrated that HEPA performance can be achieved through only mechanical filtration by using an appropriately structured meltblown nonwoven. The pressure drop across the membrane was comparable to the commercial fiberglass one. We also demonstrated that MPPS can be lowered with using smaller fibers.

Acknowledgments

The authors gratefully acknowledge the Nowovens Cooperative Research Center (NCRC) of North Carolina State University for supporting this research. They would also like to thank Dr. Rajeev Chhabra (Proctor & Gamble) and Mr. Tim Robson (Hills Inc.) for their discussions and feedback during the course of this study.

Appendix A. Supporting information

Supplementary data associated with this article can be found in the online version at http://dx.doi.org/10.1016/j.memsci.2012.09.050.

References

[1] Renuga Gopal, Satinderpal Kaur, Zuwei Maa, Casey Chanc, Seeram Ramakrishna, Takeshi Matsuura, Electrospun nanofibrous filtration membrane, J. Membr. Sci. 281 (2006) 581–586.
[2] R.S. Barhatea, Seeram Ramakrishna, Nanofibrous filtering media: filtration problems and solutions from tiny materials, J. Membr. Sci. 296 (2007) 1–8.
[3] R.S. Barhate, Chong Kian Loong, Seeram Ramakrishna, Preparation and characterization of nanofibrous filtering media, J. Membr. Sci. 283 (2006) 209–218.
[4] Darrell H. Reneker, Alexander L. Yarin, Electrospinning jets and polymer nanofibers, Polymer 49 (2008) 2387–2425.
[5] A. Gupta, C.D. Saquing, M. Afshari, R. Kotek, S.A. Khan, Porous nylon 6 fibers via a noval salt-induced electrospinning method, Macromolecules 42 (2009) 709–715.
[6] S. Talwar, A.S. Krishnan, J.P. Hinestroza, B. Pourdeyhimi, S.A. Khan, Electrospun nanofibers with associative polymer-surfactant systems, Macromolecules 43 (18) (2010) 7650–7656.
[7] C. Tang, C.D. Saquing, S.A. Khan, In situ cross-linking of electrospun poly(vinyl alcohol) nanofibers, Macromolecules 43 (2010) 630–637.
[8] C.A. Bonino, K. Efimenko, S.I. Jeong, M.D. Krebs, E. Alsberg, S.A. Khan, Three-dimensional electrospun alginate nanofiber mats via tailored charge repulsions, Small 8 (12) (2012) 1928–1936.
[9] J.L. Manasco, C.D. Saquing, C. Tang, S.A. Khan, Cyclodextrin fibers via polymer-free electrospinning, RSC Adv. 2 (9) (2012) 3778–3784.
[10] C.D. Saquing, J.L. Manasco, S.A. Khan, Electrospun nanoparticle-nanofiber composites via a novel one-step synthesis, Small 5 (2009) 944–951.
[11] Paul D. Dalton, Dirk Grafahrend, Kristina Klinkhammer, Doris Klee, Martin Moller, Electrospinning of polymer melts: Phenomenological observations, Polymer 48 (2007) 6823–6833.
[12] Robert L. Shambaugh, A macroscopic view of the melt-blowing process for producing microfibers, Ind. Eng. Chem. Res. 27 (12) (1988) 2363–2372.
[13] S.J. Russell, Handbook of Nonwovens, CRC Press, 2007.
[14] W. Albrecht, H. Fuchs, W. Kittelmann, Nonwoven Fabrics: Raw Materials, Manufacture, Applications, Characteristics, Testing Processes, Wiley, 2003.
[15] Xiao-Hong Qin, Shan-Yuan Wang, Filtration properties of electrospinning nanofibers, J. Appl. Polym. Sci. 102 (2006) 1285–1290.
[16] Zbigniew Lewandowski, Andrzej Ziabicki, Leszek Jarecki, The nonwovens formation in the melt-blown process, Fibers Text. East. Eur. 15 (5) (2007) 64–65.
[17] K.J. Choi, J.E. Spruiell, J.F. Fellers, L.C. Wadsworth, Strength properties of melt blown nonwoven webs, Polym. Eng. Sci. 28 (2) (1988) 81–89.
[18] Tien T. Wu, Robert L. Shambaugh, Characterization of the melt blowing process with laser Doppler velocimetry, Ind. Eng. Chem. Res. 31 (1) (1992) 379–389.
[19] Youngchul Lee, Larry C. Wadsworth, Effects of melt-blowing process conditions on morphological and mechanical properties of polypropylene webs, Polymer 33 (8) (1992) 1200–1209.
[20] Vishal Bansal, Robert L. Shambaugh, On-line determination of diameter and temperature during melt-lowing of polypropylene, Ind. Eng. Chem. Res. 37 (5) (1998) 1799–1806.
[21] Brian D. Tate, Robert L. Shambaugh, Modified dual rectangular jets for fiber production, Ind. Eng. Chem. Res. 37 (9) (1998) 3772–3779.
[22] Eric M. Moore, Dimitrios V. Papavassiliou, Robert L. Shambaugh, Air velocity, air temperature, fiber vibration and fiber diameter measurements on a practical melt blowing die, Int. Nonwovens J. Fall (2004) 43–53.

[23] Jessica H. Beard, Robert L. Shambaugh, Brent R. Shambaugh, David W. Schmidtke, On-line measurement of fiber motion during melt blowing, Ind. Eng. Chem. Res. 46 (22) (2007) 7340–7352.
[24] Holly M. Krutka, Robert L. Shambaugh, Dimitrios V. Papavassiliou, Effects of temperature and geometry on the flow field of the melt blowing process, Ind. Eng. Chem. Res. 43 (15) (2004) 4199–4210.
[25] Holly M. Krutka, Robert L. Shambaugh, V. Dimitrios, Papavassiliou analysis of a melt-blowing die: comparison of CFD and experiments, Ind. Eng. Chem. Res. 41 (2002) 5125–5138.
[26] Holly M. Krutka, Robert L. Shambaugh, Dimitrios V. Papavassiliou, Effects of die geometry on the flow field of the melt-blowing process, Ind. Eng. Chem. Res. 42 (22) (2003) 5541–5553.
[27] M.W. Milligan, F. LU, R.R. Buntin, L.C. Wadsworth, The use of crossflow to improve nonwoven melt-blown fibers, J. Appl. Polym. Sci. 44 (1992) 279–288.
[28] Y. Lee, L.C. Wadsworth, Structure and filtration properties of melt blown polypropylene webs, Polym. Eng. Sci. 30 (22) (1990) 1413–1419.
[29] Arthur G., Russell Co., 2009, 〈http://www.arthurgrussell.com/nanofiber.shtml〉.
[30] G.F. Ward, Meltblown nanofibres for nonwoven filtration applications, Filtr. Sep. 38 (9) (2001) 42–43.
[31] Anthony S. Fabbricante, et al., US Patent 5,679,379, 1997.
[32] Christopher J. Ellison, Alhad Phatak1, David W. Giles, Christopher W. Macosko, Frank S. Bates, Melt blown nanofibers: fiber diameter distributions and onset of fiber breakup, Polymer 48 (2007) 3306–3316.
[33] Dwight T. Lahkamp, et al., US Patent 3,825,379, 1974.
[34] John W. Harding, et al., US Patent 3,825,380, 1974.
[35] Martin A. Allen, et al., US Patent 5,605,706, 1997.
[36] Kui-Chiu Kwok, et al., US Patent 5,904,298, 1999.
[37] Vishal Bansal, et al., US Patent 6,776,858 B2, 2004.
[38] James E.Brang, et al., US Patent 2008/0023888 A1, 2008.
[39] TSI 3160 Manual, 2002.
[40] Irwin Hutten, Handbook of Non-Woven Filter Media, Elsevier Sci. & Tech. Books, 2007.
[41] Akshaya Jena, Krishna Gupta, Characterization of pore structure of filtration media, Fluid Part. Sep. J. 14 (3) (2002) 227–241.
[42] Akshaya Jena, Krishna Gupta, Liquid extrusion techniques for pore structure, evaluation of nonwovens, Int. Nonwovens J. (Fall) (2003) 45–53.
[43] Stanislav Petrik, Miroslav Maly, Production nozzle-less electrospinning nanofiber technology, in: Proceedings of the 2009 Fall MRS Symposium, Boston, MA, Nov 30–Dec 4, 2009.
[44] Jing Wang, et al., Figure of merit of composite filter with micrometer and nanometer fibers, Aerosol, Sci. Technol. 42 (2008) 722–728.
[45] Jing Wang, et al., Investigation of the figure of merit for filters with a single nanofiber layer on a substrate, J. Aerosol Sci. 39 (2008) 323–334.
[46] Albert Podgorski, et al., Application of nanofibers to improve the filtration efficiency of the most penetrating aerosol particles in fiberous filters, Chem. Eng. Sci. 61 (2006) 6804–6815.
[47] Seetha S. Manickam, Jeffrey R. McCutcheon, Characterization of polymeric nonwovens using porosimetry, porometry and X-ray computed tomography, J. Membr. Sci. 407– (408) (2012) 108–115.